

## Sorption of $\beta$ -naphthalene sulfonic acid by weak base anion exchangers as controlled by alkyl chain length of the amine functional group

Yue Sun<sup>a,\*</sup>, Deqiang Yin<sup>a</sup>, Jintao Duan<sup>b</sup>, Rajendra Prasad Singh<sup>a</sup>

<sup>a</sup>School of Civil Engineering, Southeast University, Nanjing, 210096, China, Tel. +86-25-83790757, Fax +86-25-83790757, email: sycyseu@163.com (Y. Sun), ydqmail@163.com (D. Yin), 0703160124@163.com (J. Duan), rajupsc@seu.edu.cn (R.P. Singh)

<sup>b</sup>Anhui Provincial Architectural Design and Research Institute, Hefei, 230002, China, Tel. +86-551-63411241

Received 14 March 2016; Accepted 1 July 2016

### ABSTRACT

Weak base anion exchangers are promising for decontamination of aromatic ionizable organic compounds (AIOCs) from industrial wastewaters. However, the effect of alkyl chain length of an amine functional group of resins on decontamination process has rarely been clarified to the best of our knowledge. In the present study, a commercially available weak base anion exchange resin D301 and two newly synthesized ones AEC-2 and AEC-4 with a varying alkyl chain length of amine functional groups (derived from dimethylamine, diethylamine and dibutylamine, respectively) were used for adsorption of  $\beta$ -naphthalene sulfonic acid (NSA). Adsorption isotherms and influence of solution pH, temperature, time and coexisting competitive inorganic salt ( $\text{Na}_2\text{SO}_4$ ) on adsorption behavior were investigated and the column adsorption-regeneration tests were carried out. Results showed that adsorption selectivity for NSA over sulfate increased with increasing the alkyl chain length in the high saline water. But the sorption velocity decreased to a moderate extent with increasing the alkyl chain length. Thermodynamic parameters indicate that adsorption is an exothermic and spontaneous process, and NSA adsorption onto AEC-4 is an enthalpy-driven process, while that of D301 as well as AEC-2 is an enthalpy- and entropy-driven simultaneous process. Further, results of column tests validate long alkyl chain enhancing the sorption selective for NSA and suggest the sorption process can be reversible.

*Keywords:*  $\beta$ -Naphthalene sulfonic acid; Anion exchange resin; Adsorption; Selectivity

### 1. Introduction

Numerous environmentally significant synthetic aromatic compounds, also known as aromatic ionizable organic compounds (AIOCs), can be ionized at amiable pH conditions and thus have a tendency to enter surface and ground water, posing potential human health and ecological risks [1–3]. As a group of the widespread AIOCs, aromatic sulfonic acids (ASAs) and their salt forms are commonly used as intermediates in the production of pharmaceuticals, ion exchange resins, pesticides, wetting agents, optical brighteners and synthetic dyes [4–6]. Since ASAs are highly soluble in water, they often present in industrial wastewaters at high levels, and cause a great threat to

the environment once discharged into the receiving water system [4]. Due to their sulfonated nature, ASAs are resistant to microbial breakdown and have been described as poorly biodegradable or even non-biodegradable [7–9]. In recent years, a number of different procedures, such as complex extraction, advanced oxidation, adsorption, etc., have already been proposed for remediation of ASAs [10–16]. Among them, adsorption is one of the most effective physical processes for removal of organic pollutants from contaminated waters. Because of their high solubility, ASAs are not able to be effectively removed by activated carbon and conventional polymeric sorbents except for polymeric weak base anion exchangers, which show feasible sorption and regeneration properties towards ASAs [17]. However, most industrial wastewaters accompanied by the production of ASAs by neutralization after the sulfonation process of aromatic substrates, contain not only

\*Corresponding author.

high-level ASAs but also excessive  $\text{Na}_2\text{SO}_4$  or other inorganic salts, which inevitably compete for the active sites, resulting in a significant decrease in adsorption capacity and efficiency of weak base anion exchangers [18]. For instance, the commercial weak base anion exchange resin D301 was used for removal of ASAs such as benzenesulfonic acid, where results showed that the addition of about 0.5%  $\text{Na}_2\text{SO}_4$  in mass could greatly weaken the selectivity of D301, and the adsorption capacity of D301 towards benzenesulfonic acid decreased by more than 60% [17]. To overcome this drawback of the conventional exchanger, some researchers initiated the work on the effect of the matrix structure of a resin on the sorption selectivity and prepared the hyper-crosslinked polymeric resin with weak base exchange group for selective removal of ASAs from wastewaters along with high level of inorganic salts [19,20]. Although hyper-crosslinked polymeric resin had large specific surface area and rich microporous characteristics, the adsorption capacity of such resin was still limited due to its low anion exchange capacity. Moreover, the high price of about six times of the common anion exchanger caused the hyper-crosslinked resin with less attractive for field application [19]. In fact, besides framework structure, functional group of an adsorbent plays a key role on its properties [21]. Unfortunately, up to date, scarce work related to weak base anion exchange group of a resin enhancing selective adsorption of ASAs from saline wastewaters has been reported.

Therefore, main objective of the current work is to evaluate the sorption behavior of ASAs on different weak base anion exchange resins through batch and column approaches, and especially explore the relationship between resin selectivity and alkyl chain length of the amine group on resins.  $\beta$ -Naphthalene sulfonic acid (NSA) is selected as a representative of ASAs due to its environmental significance and widespread occurrence in wastewaters.

## 2. Experimental

### 2.1. Materials

Macroporous chloromethylated polystyrene-divinylbenzene (Cl-PS-DVB) beads holding 6% of crosslinking degree and 18% of chloride content, as well as commercial weak base anion exchanger D301 were obtained from Zhengguang Co., Ltd (Zhejiang, China).  $\beta$ -Naphthalene sulfonic acid (NSA) was purchased from the Aladdin Industrial Corporation (Shanghai, China). Diethylamine and dibutylamine as well as other reagents such as  $\text{Na}_2\text{SO}_4$ , HCl,  $\text{H}_2\text{SO}_4$ , NaOH, ethanol and benzene were purchased from Nanjing Reagent Co., Ltd (Jiangsu, China). All the chemicals were of analytical grade and used without further purification.

### 2.2. Resin preparation and characterization

In a 250-mL three-necked flask equipped with a mechanical stirrer, a thermometer and a reflux condenser, 30 g of Cl-PS-DVB beads were swollen in 60 g of benzene at 303 K for 12 h, and then the swollen polymer particles were filtered out of the suspension. A solution comprised

of 25 g of diethylamine and 40 g of ethanol was then gradually added, and the mixture was stirred at 318 K for 10 h. Finally, the weak base anion exchanger AEC-2 was obtained through the filtration of residual diethylamine. AEC-4 resin was synthesized with similar procedure except for the dibutylamine dosage adjusted to 40 g.

Prior to use, each of the resins was loaded into a column and washed with 4% diluted HCl, deionized water followed by 4% diluted NaOH solution. Afterwards, the resin beads were washed to neutral pH with deionized water. In order to minimize the disturbing effect of quaternary ammonium group bound onto the polymeric matrix, each resin was subjected to 3 cycles of sorption-desorption process of NSA from aqueous solution according to a previous procedure [19]. The sorption-desorption process was described briefly as follows: a synthetic solution containing 5000 mg/L NSA flew through the column slowly to ensure the complete exhaustion of the resin. After sorption, 8% NaOH solution was used as eluate reagent at 318 K until NSA was undetectable in desorption effluent, and then the resin beads were thoroughly washed with deionized water to neutral pH. Finally, resin beads were extracted for 5 h with ethanol and dried at 318 K under vacuum to constant weight.

Specific surface area and pore structure of the resins were determined by BET methods through nitrogen adsorption and desorption curves at 77 K using an automatic surface area analyzer (Micromeritics ASAP-2020, USA). Infrared spectra of Cl-PS-DVB beads and newly synthesized resins were taken from a Nicolet 5700 FTIR spectrometer (Madison, USA) with a pellet of powdered potassium bromide and adsorbent.

### 2.3. Batch adsorption experiments

Batch adsorption studies were carried out in 250 mL glass flasks. Dry resin (0.100 g) was introduced to a 100 mL solution containing known initial concentration of NSA. The flasks were completely sealed and placed in a thermostatic oscillator (Guangming Experimental Instrument Co., China) at the desired temperature and shaken at 150 rpm for 24 h to ensure the adsorption process reaching equilibrium. Diluted  $\text{H}_2\text{SO}_4$  or NaOH solution was used to adjust the solution pH and  $\text{Na}_2\text{SO}_4$  was introduced into the flask before adsorption when necessary. As for kinetics study, 0.500 g of adsorbent and 500 mL of NSA solution with an initial concentration of 1000 mg/L were introduced into a 1000 mL conical flask quickly and shaken at a speed of 150 rpm at 303 K continuously, and 0.5 mL solution at various time intervals was sampled from the flasks to determine sorption kinetics. The concentrations of NSA before and after adsorption were detected using a UV1800 spectrophotometer (Jinghua Scientific Instruments, China). The adsorption amounts of the sorbents at equilibrium ( $Q_e$ , mg/g) were calculated by the following equation:

$$Q_e = (C_0 - C_e)V / W \quad (1)$$

where  $C_0$  and  $C_e$  are the initial and equilibrium NSA concentrations respectively (mg/L),  $W$  is the mass of resin (g) and  $V$  is the volume of solution (L).

#### 2.4. Column tests

Column experiments were carried out with a glass column (18 mm in diameter) equipped with a water bath to maintain a constant temperature. A 10 mL portion of resin was packed into the column for test. A synthetic solution containing 8000 mg/L NSA and 10% Na<sub>2</sub>SO<sub>4</sub> was employed as the feeding solution and pumped down-flow through the column at 303 K. After adsorption, the exhausted resin bed was subjected to regeneration by 2 bed volumes (BV) 8% NaOH solution followed by 3 BV deionized water at 318 K. The hydrodynamic conditions, i.e., a superficial liquid velocity (SLV) of 0.12 m/h and an empty bed contact time (EBCT) of 20 min were identical for the column adsorption runs. As for the regeneration test, they were determined as 0.04 m/h and 60 min, respectively.

### 3. Results and discussion

#### 3.1. Characterization of resins

The FTIR spectra results for sorbent characterization are presented in Fig. 1. As compared with Cl-PS-DVB, the new peaks at 1089 cm<sup>-1</sup> of AEC-2 and AEC-4 demonstrated that C-N existed in the synthesized resins [16], which showed that the amination process was accomplished.

The general properties of the tested resins are listed in Table 1. Note that BET surface area of each resin was in the same level, but the exchange capacity decreased with increasing alkyl chain length of the amine group on the resins.

#### 3.2. Effect of pH on adsorption

pH is an important controlling parameter in most of the adsorption processes. The pH-dependent trend of the sorption capacity at initial NSA concentration of 1000 mg/L is shown in Fig. 2. More favorable adsorption of all the tested

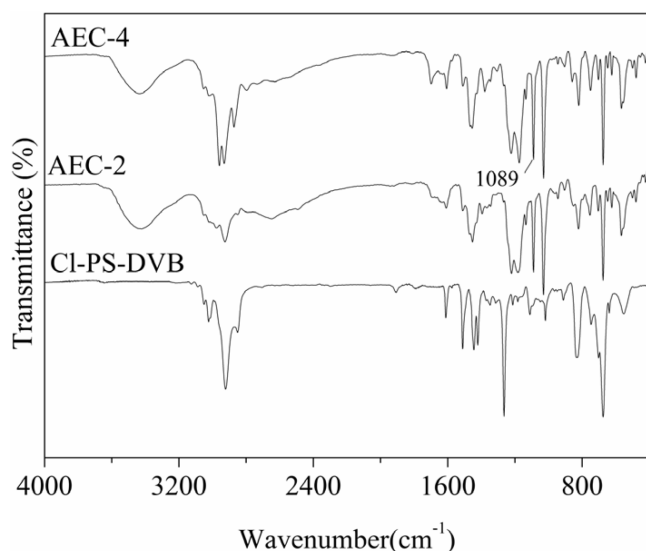


Fig. 1. FTIR spectra of AEC-2, AEC-4 and Cl-PS-DVB beads.

Table 1  
Characteristics of resins

Property	D301	AEC-2	AEC-4
Matrix structure	PS-DVB	PS-DVB	PS-DVB
Cross-link density (%)	6	6	6
Functional group	-N(CH <sub>3</sub> ) <sub>2</sub>	-N(C <sub>2</sub> H <sub>5</sub> ) <sub>2</sub>	-N(C <sub>4</sub> H <sub>9</sub> ) <sub>2</sub>
BET surface area (m <sup>2</sup> /g)	26.9	23.4	29.7
Average pore diameter (nm)	42.6	24.5	37.3
Total anion exchange capacity (mmol/g)	3.85	3.25	2.89
Quaternary ammonium group (mmol/g)	0.31	0.18	0.22

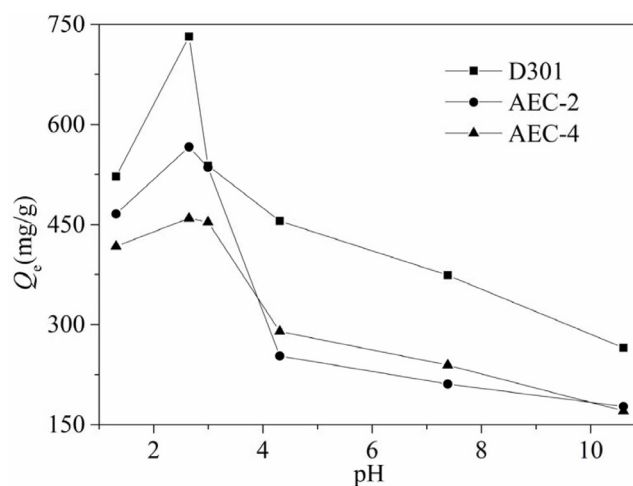


Fig. 2. Effect of solution pH on the adsorption of NSA onto resins.

resins was observed at acidic medium and the optimum pH value was about 2.6. At acidic pH, the amine groups on the resins could be protonated and subsequently interact with the negatively charged NSA anions through an electrostatic attraction mechanism. Higher solution pH was unfavorable for protonation of amine group and resulted in a lower sorption capacity. The similar phenomenon also observed and well explained by X-ray photoelectron spectroscopy analysis in studying some nitrogen-containing materials such as aminated hyper-crosslinked resin and chitosan-coated polymer for adsorption of aromatic sulfonates and humic acid [17,22]. As the solution pH was lower than the optimal value, decrease in sorption capacity might be due to the

addition of sulfate anions for pH adjustment. In fact, sulfate anions could also be sorbed on the resins by electrostatic interaction with the protonated amine groups and lead to the competitive sorption with NSA anions [19]. Additionally, the pKa value of NSA was about 2.7, therefore the proportion of neutral NSA molecular state was increased in a strongly acidic solution, which was unfavorable for the sorption through an electrostatic attraction mechanism [23].

### 3.3. Equilibrium adsorption and selectivity

Generally, some inorganic ions often dissolved in industrial wastewaters are environmentally friendly. But, they as competing ions could strongly interfere with adsorption process of AIOCs, which would result in inefficiency. Therefore, adsorption ability and selectivity of a resin required proper evaluation for the practical application. Fig. 3 illustrates the adsorption isotherms of NSA on resins from aqueous solution with or without addition of  $\text{Na}_2\text{SO}_4$ . To characterize the adsorption equilibrium of NSA by the resins, the data were analyzed using Langmuir (Eq. (2)) and Freundlich (Eq. (3)) equilibrium models.

$$\frac{C_e}{Q_e} = \frac{C_e}{Q_m} + \frac{1}{(K_L Q_m)} \quad (2)$$

$$\ln Q_e = \ln K_F + \left(\frac{1}{n}\right) \ln C_e \quad (3)$$

where,  $Q_e$  is the equilibrium adsorption capacity of the adsorbent (mg/g);  $C_e$  is the equilibrium concentration of NSA (mg/L); and  $K_F$ ,  $n$ ,  $Q_m$  and  $K_L$  are the characteristic constants. With obtained data of  $Q_e$  and  $C_e$ , all the isotherm parameters could be determined by plotting  $C_e/Q_e$  against  $C_e$  as well as  $\ln Q_e$  versus  $\ln C_e$  based on Eqs. (2) and (3), respectively. The correlative relevant parameters and correlation coefficients ( $R^2$ ) of Langmuir and Freundlich isotherm equations are listed in Table 2.

It is clear from the Table 2, that Langmuir equations were more reliable than Freundlich equations because all the correlation factors ( $R^2$ ) of the former were larger than those of the latter. As expected, NSA adsorption onto all the resins obviously decreased with  $\text{Na}_2\text{SO}_4$  addition due to competitive adsorption between sulfate and NSA anion. A significant observation from sorption isotherms was the different behaviors of the three resins dependent on the coexisting  $\text{Na}_2\text{SO}_4$  concentration levels. In the absence of  $\text{Na}_2\text{SO}_4$ , the adsorption capacity towards NSA decreased in the following order: D301 > AEC-2 > AEC-4, which was consistent with the content of functional groups on resins. Contrarily, in binary system at 1%  $\text{Na}_2\text{SO}_4$ , the sorption amount order was AEC-2 > AEC-4 > D301, while when  $\text{Na}_2\text{SO}_4$  concentration increased to 5%, that changed into AEC-4 > AEC-2 > D301.

Generally, two sorption mechanisms namely  $\pi$ - $\pi$  dispersion interaction between aromatic ring of the solute molecule and the PS-DVB matrix of the resin and electrostatic interaction resulting from charged functional groups govern the adsorption of AIOCs on polymeric anion exchangers [24,25]. Taken into account their same PS-DVB matrix and similar surface area, different adsorption performance of

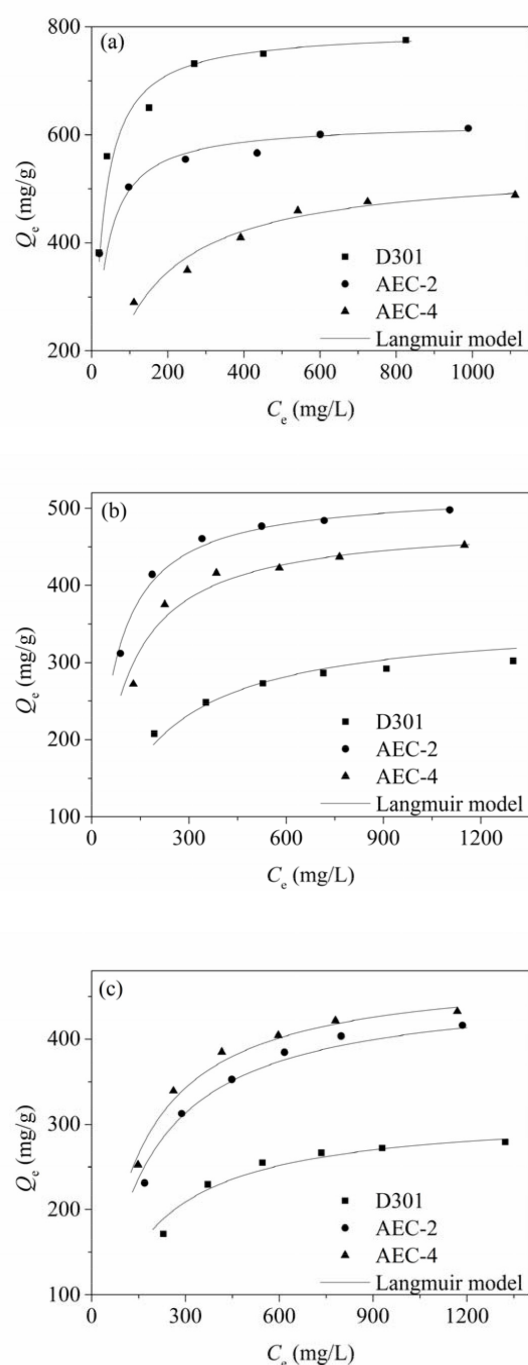


Fig. 3. Sorption isotherms of NSA on resins at 303 K and  $\text{Na}_2\text{SO}_4$  in solution controlled at (a) 0%, (b) 1%, and (c) 5%, respectively.

D301, AEC-2 and AEC-4 could be attributed to the chemical structure of the sorbents. It was reported that both basic strength and hydrophobicity of the amination reagent for synthesis of ion exchangers could affect the sorption selectivity towards organic anion [26,27]. The values of logarithmic relations between the octanol/water partition coefficient  $K_{OW}$  which is a parameter for hydrophobicity and  $\text{p}K_b$  as an indicator for basic strength of three amine reagents used for functional reaction of the resins are listed in Table 3.

Table 2  
Fitting results with Freundlich and Langmuir isotherm models for NSA

Resin	Na <sub>2</sub> SO <sub>4</sub> (%)	Freundlich equation			Langmuir equation		
		<i>n</i>	<i>K<sub>F</sub></i>	<i>R</i> <sup>2</sup>	<i>Q<sub>m</sub></i> (mg/g)	<i>K<sub>L</sub></i> (L/g)	<i>R</i> <sup>2</sup>
D301	0	5.734	260.50	0.8798	794.7	42.47	0.9996
	1	5.076	76.56	0.9430	358.3	6.15	0.9961
	5	3.761	44.45	0.8498	316.1	6.49	0.9963
AEC-2	0	8.224	274.32	0.9562	622.9	40.13	0.9991
	1	5.659	153.65	0.8632	521.4	19.40	0.9998
	5	3.472	57.68	0.8924	462.7	6.98	0.9967
AEC-4	0	4.060	92.07	0.9592	541.8	8.83	0.9976
	1	4.755	109.54	0.8179	484.0	12.62	0.9987
	5	3.954	78.03	0.8874	478.2	8.84	0.9989

Data from Table 3 reveal that dimethylamine had the lowest hydrophobicity and basic strength among three functional reagents. As a result, D301 showed the lowest adsorption capacity of NSA in the presence of Na<sub>2</sub>SO<sub>4</sub>, even though its exchange capacity was much higher than that of AEC-2 as well as AEC-4. Dibutylamine was more hydrophobic and alkaline than diethylamine, its derived resin AEC-4 should possess a higher adsorption selectivity for NSA. However, the limited exchange capacity of AEC-4 resulted in its lower sorption capacity than AEC-2 at the moderate Na<sub>2</sub>SO<sub>4</sub> level of 1%, while when the saline concentration increased to 5%, more coexisting sulfate could lead to stronger competitive adsorption with NSA anion, therefore better sorption ability of AEC-4 than AEC-2 was observed. Additionally, it had been reported that increasing the distance between active exchange sites on strongly basic anion exchangers was favorable for the selectivity for monovalent inorganic anions such as perchlorate, nitrate and perchlorate over divalent ions such as sulfate [28,29]. This might be a more important reason for the sorption selectivity trend toward NSA of different sorbents. In fact, sulfate behaves as a divalent anion, which needed to be adsorbed with two contiguous active sites on the resin, thus, when the spacing between active sites became large by increasing the alkyl chain length of the amine group on resins, sulfate could not be adsorbed well. However, monovalent ions such as NSA were still adsorbed in the resin because it needed only one active sorption site. This might reduce the affinity of the resin to sulfate, if the alkyl chain of amine functional

group was long then it was harder for such divalent ion as sulfate to attach to the resins.

In order to quantify the selectivity of the three resins, the distribution ratio *K<sub>d</sub>* (in mL/g) was calculated using the following equation [17]:

$$K_d = \frac{\text{mg of NSA} / \text{1g of dry resin}}{\text{mg of NSA} / \text{1mL of dry resin}} \quad (4)$$

The resulting *K<sub>d</sub>* values of the tested resins at different initial NSA concentration are listed in Table 4. Results reveal that, at the identical amount of Na<sub>2</sub>SO<sub>4</sub> addition, the distribution ratio values decreased with the initial NSA concentration increasing for all the resins. Both the synthesized resins showed better sorption selectivity towards NSA. For example, when initial NSA concentration was 400 mg/L, the *K<sub>d</sub>* values of AEC-2 and AEC-4 were 227% and 97% at Na<sub>2</sub>SO<sub>4</sub> concentration of 1%, while 82% and 128% at Na<sub>2</sub>SO<sub>4</sub> concentration of 5% higher than those of D301, respectively. The results also suggested that AEC-2 was more suitable for NSA removal from wastewater with moderate concentration of sulfate, and AEC-4 could be used for treatment of wastewater containing relatively high level of sulfate.

Table 3  
Characteristics of the functional reagents of the resins

Property	Dimethylamine	Diethylamine	Dibutylamine
log <i>K<sub>OW</sub></i> <sup>a</sup>	-0.38	0.58	2.83
p <i>K<sub>b</sub></i> <sup>b</sup>	3.27	3.16	2.75

<sup>a</sup>Obtained from X.K. Wu, Ed. Table of Environmental Data of Organic Compounds, 2009.

<sup>b</sup>Taken from D.R. Lide, Ed. Handbook of Chemistry and Physics, 2003.

Table 4  
Effect of Na<sub>2</sub>SO<sub>4</sub> concentration on NSA distribution coefficient (*K<sub>d</sub>*, mL/g)

Resin	Na <sub>2</sub> SO <sub>4</sub> (%)	Initial NSA concentration (mg/L)		
		400	800	1200
D301	1	1076.9	517.0	321.2
	5	748.4	466.6	292.8
AEC-2	1	3517.3	1352.4	674.9
	5	1364.6	786.8	505.6
AEC-4	1	2116.5	1081.1	571.7
	5	1706.2	924.4	540.6

### 3.4. Effect of temperature and thermodynamics

The NSA adsorption isotherms at different temperatures on the three resins are presented in Fig. 4a–c. The equilibrium adsorption capacities decreased with increasing temperature, which indicated that the low temperature was beneficial to the adsorption.

As the sorption feature followed the Langmuir model, the enthalpy change ( $\Delta H$ ) and entropy change ( $\Delta S$ ) herein could be calculated based on the following equation [30]:

$$\ln K_L = \Delta S / R + (-\Delta H / RT) \quad (5)$$

where  $K_L$  is the constant of the well fitting Langmuir equation,  $R$  is the gas constant and  $T$  is the absolute temperature.  $\Delta H$  and  $\Delta S$  were then obtained from the slope and intercept of the line plotted by  $\ln K_L$  versus  $1/T$ . Some of the plotted lines are shown in Fig. 5. The free energy change ( $\Delta G$ ) could be measured with the Gibbs equation [30]:

$$\Delta G = -RT \ln K \quad (6)$$

As presented in Table 5, exothermic adsorption processes were testified by the negative values of all the enthalpy changes. The larger absolute values of the changes in adsorption enthalpy of AEC-2 and AEC-4 revealed that the interaction between NSA and the newly synthesized resins was stronger than that between NSA and D301 due to the enhanced basic strength and hydrophobicity of the functional groups on AEC-2 and AEC-4. The free energy changes were always negative, which proved that the adsorption processes of NSA on employed resins were all spontaneous. An important observation from Table 5 was the different entropy change characteristics of the three resins. The entropy change during the adsorption of NSA on AEC-4 was negative, but it was positive for D301 as well as AEC-2. Usually, adsorption is an entropy decreasing process because the activity of adsorbate molecules on adsorbents is weaker than those in the aqueous solution. The entropy increasing phenomenon observed for D301 and AEC-2 might be attributed to effect of the water molecules. In aqueous solution, water molecules were strongly attached to the polar functional groups on the resin and water clusters were built up on these groups by hydrogen bond interaction. The effective adsorption for NSA was required for the destruction of water clusters and water molecules would turn away from solid surface in the form of water clusters to the solution in a more disorderly free water state. This process would bring chaos to the system and lead to the increase of entropy [31]. In comparison with D301 and AEC-2, AEC-4 had a more hydrophobic functional group which interacted with water molecule weakly, so its entropy change in the sorption process was still negative. This phenomenon also suggested that NSA adsorption onto AEC-4 was an enthalpy-driven process, while D301 as well as AEC-2 was an enthalpy- and entropy-driven simultaneous process.

### 3.5. Adsorption kinetics

Adsorption kinetics is one of the most important characteristics which represent the adsorption efficiency. Fig. 6

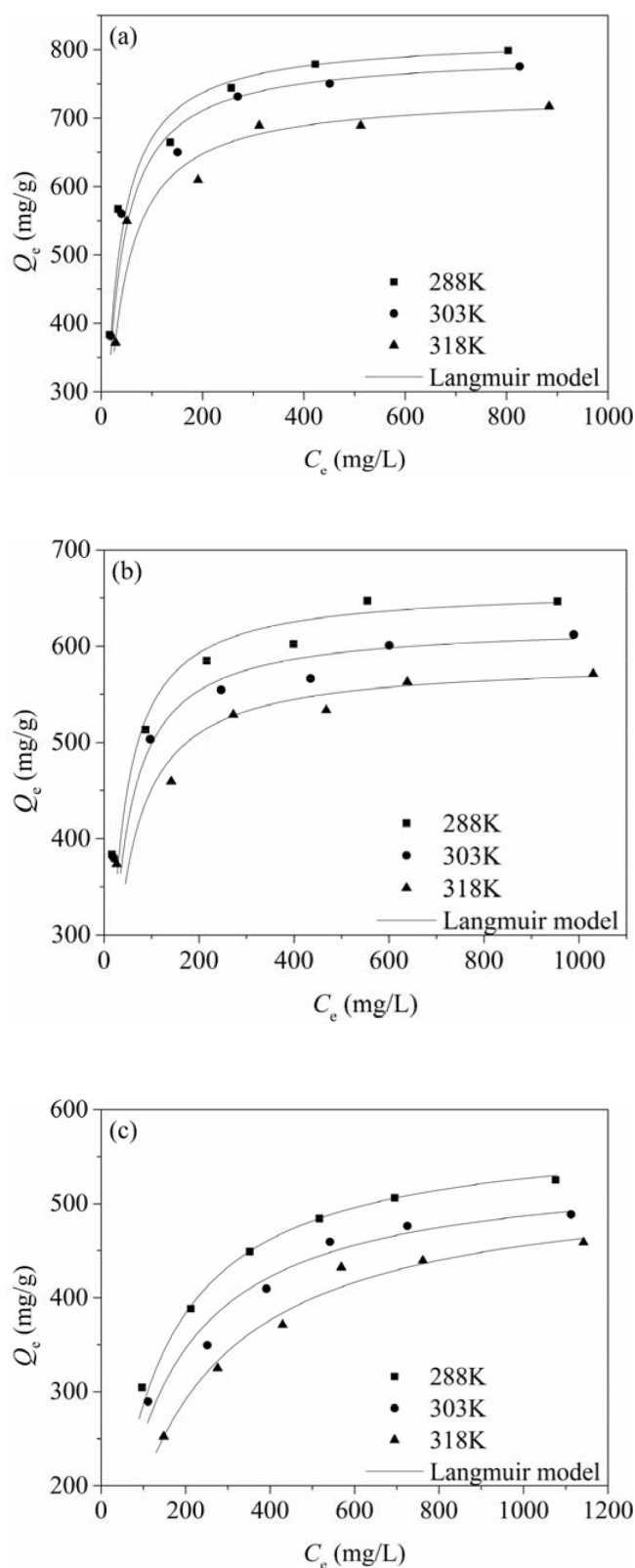


Fig. 4. Effect of temperature on sorption of NSA onto (a) D301, (b) AEC-2 and (c) AEC-4.

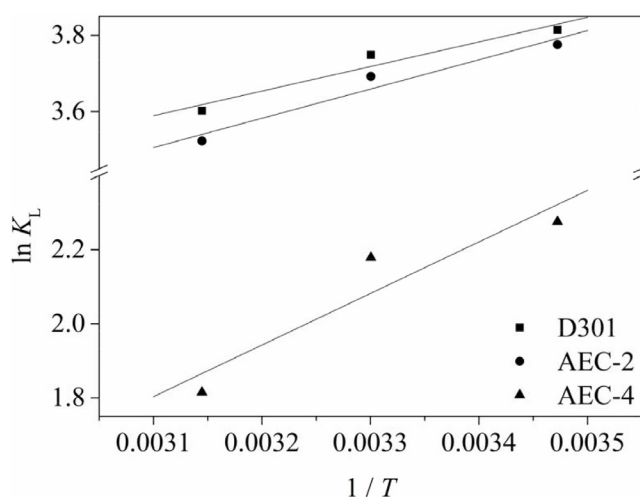


Fig. 5. Plots of  $\ln K_L$  vs.  $1/T$  for determination of  $\Delta H$  and  $\Delta S$  during NSA sorption on resins.

Table 5  
Calculated thermodynamic parameters for adsorption of NSA onto resins

Resin	$\Delta H$ (kJ/mol)	$\Delta S$ (J/mol K)	$\Delta G$ (kJ/mol)		
			288 K	303 K	318 K
D301	-5.35	13.25	-9.13	-9.44	-9.52
AEC-2	-6.37	9.41	-9.04	-9.30	-9.31
AEC-4	-11.59	-20.92	-5.45	-5.49	-4.80

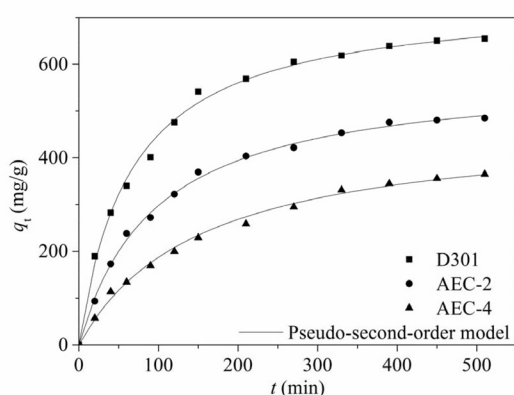


Fig. 6. Kinetic curves for the adsorption of NSA on resins at 303 K.

shows the adsorption behavior of NSA onto the resins at initial concentration of 1000 mg/L as a function of adsorption time. The pseudo-first-order (Eq. (7)), pseudo-second-order (Eq. (8)) and Elovich (Eq. (9)) equations were used to further describe the kinetic behaviors of NSA adsorbing onto the resins [32].

$$\ln(1 - q_t / Q_e) = -k_1 t \quad (7)$$

$$\frac{t}{q_t} = \frac{t}{Q_e} + \frac{1}{k_2 Q_e^2} \quad (8)$$

$$q = \left(\frac{1}{\beta}\right) \ln(\alpha\beta) + \left(\frac{1}{\beta}\right) \ln(t) \quad (9)$$

where,  $Q_e$  and  $q_t$  are the adsorption capacity (mg/g) at equilibrium and at time  $t$ , respectively, while  $k_1$  ( $\text{min}^{-1}$ ) and  $k_2$  ( $\text{g}/(\text{mg}\cdot\text{min})$ ) are the rate constants for the first- and second-order equations, respectively. For Elovich equation,  $\alpha$  is the initial adsorption rate ( $\text{mg}/(\text{g}\cdot\text{min})$ ), and  $\beta$  is the desorption constant ( $\text{g}/\text{mg}$ ). The correlation parameters and coefficients ( $R^2$ ) data are presented in Table 6.

Because of relatively low  $R^2$  values and the calculated equilibrium sorption capacities ( $Q_{e,\text{cal}}$ ) are inconsistency with the experimental sorption capacities ( $Q_{e,\text{exp}}$ ), thus it could be concluded from Table 6 that the pseudo-first-order model was not well fitted for modelling of kinetic data. The  $R^2$  values greater than 0.98 for the tested sorption system suggested that the data fitted well the Elovich equation, and the adsorption would be a chemical process [33]. The values of  $Q_{e,\text{cal}}$  were much closer to  $Q_{e,\text{exp}}$  and the highest values of  $R^2$ , suggested that the pseudo-second-order model could explain best the adsorption processes onto all the resins, and the sorption processes could be controlled by chemical adsorption or chemisorption involving valence forces through sharing or exchange of electrons between the two phases involved [34]. Similarly, previous studies showed that the pseudo-second-order kinetic model was often applied with success to describe the kinetics of adsorption process of ionizable organic compounds on anion exchangers from aqueous media [35–38]. Concerning to the pseudo-second-order rate constant, the value of  $k_2$  was decreased in the following order: D301 > AEC-2 > AEC-4. In other words, increasing the alkyl chain length of the amine group could result in a decrease in the sorption rate. Nevertheless, the  $k_2$  values of the three resins were of the same order of magnitude, suggesting that the tested resins had the approximate kinetic properties.

### 3.6. Column adsorption and regeneration

Fig. 7 illustrates an effluent history of a separate fixed-bed column packed with each resin for a simulated solution containing 8000 mg/L NSA and 10% competing  $\text{Na}_2\text{SO}_4$ , which was based on the analysis results of a waste stream from the  $\beta$ -naphthol production process in a chemical plant in Inner Mongolia Autonomous Region (China).

As shown in Fig. 7, NSA could be efficiently removed by D301, AEC-2 and AEC-4 within 9, 13 and 15 BV respectively before a significant breakthrough occurred, and NSA content in effluent was less than 40 mg/L on average for each resin. NSA broke through quickly on the commercial exchanger D301 resulting from the strongly competitive effect of the coexisting sulfate radical. While AEC-2 and AEC-4 exhibited more satisfactory column performance, which could be reasonably attributed to their enhanced selectivity towards NSA.

To investigate the regenerability of the NSA loaded resins, the exhausted resin columns were then regenerated first using 2 BV of 8% NaOH solution, followed by rinsing

Table 6  
Kinetic parameters for adsorption of NSA onto resins at 303 K

Resin	$Q_{e,exp}$	Pseudo-first-order model			Pseudo-second-order model			Elovich equation		
		$10^3 k_1$	$Q_{e,cal}$	$R^2$	$10^5 k_2$	$Q_{e,cal}$	$R^2$	$\alpha$	$10^3 \beta$	$R^2$
D301	731.7	3.99	454.2	0.9364	2.06	743.5	0.9989	20.85	6.00	0.9829
AEC-2	566.4	3.61	402.8	0.9508	1.80	582.4	0.9985	12.78	7.78	0.9931
AEC-4	459.5	2.99	381.7	0.9827	1.38	473.5	0.9943	7.06	9.93	0.9844

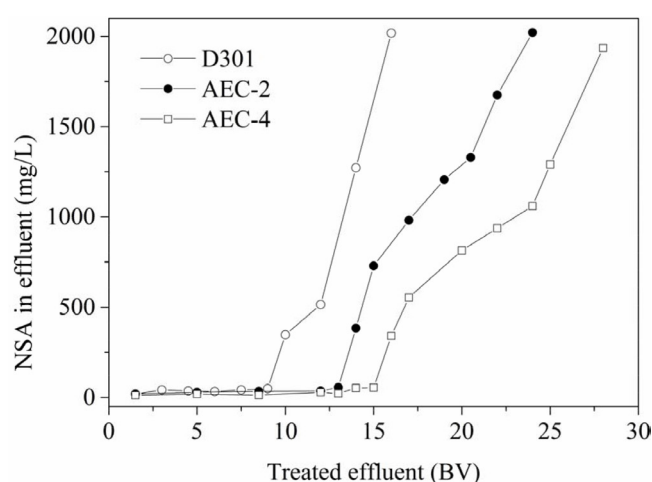


Fig. 7. Breakthrough curves of NSA adsorbed by three separate column beds packed with different resins.

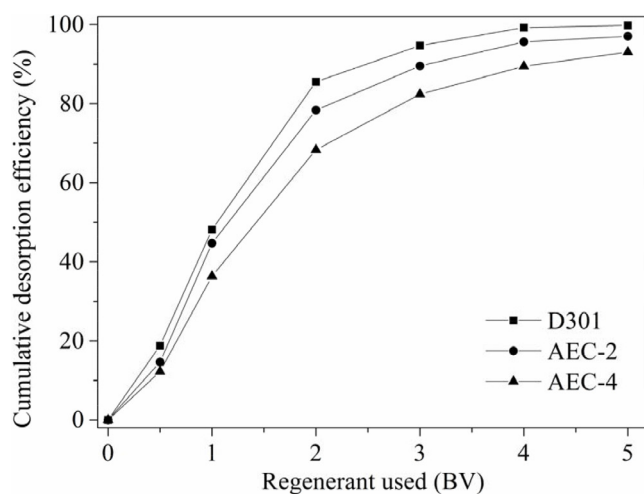


Fig. 8. Regeneration of the exhausted column beds packed with different resins.

with 3 BV of deionized water at 313 K and the results are depicted in Fig. 8.

It is clear from the Fig. 8, that increasing the alkyl chain length of the amine group was unfavorable for the desorption performance of the resins. However, NSA loaded onto the each resin was effectively eluted with the corresponding desorption efficiency exceeding 93% within total 5 BV

regenerant wash, which suggests that the sorption of NSA on the tested resins could be reversible.

#### 4. Conclusion

A commercially available weak base anion exchange resin D301 and two newly synthesized ones namely AEC-2 and AEC-4, were used for adsorption of  $\beta$ -naphthalene sulfonic acid (NSA) as a typical representative of aromatic sulfonic acids (ASAs). These resins differed in the alkyl chain length of the secondary amine used for the amination of resins, viz. dimethylamine, diethylamine and dibutylamine for D301, AEC-2 and AEC-4, respectively. D301 was found to be the best option for NSA adsorption from aqueous solution without any inorganic salt, and AEC-2 had the highest sorption ability towards NSA in water with moderate concentration of  $\text{Na}_2\text{SO}_4$ , while AEC-4 showed the best adsorption capacity for NSA in the presence of relatively high level of  $\text{Na}_2\text{SO}_4$ . This trend suggested that increasing alkyl chain length of amine functional groups could effectively improve the adsorption selectivity for NSA of the resin. For all the tested resins, high desorption rate could be achieved by NaOH aqueous solution, which indicated that the sorption of NSA was a reversible process.

#### Acknowledgements

We greatly acknowledge the financial support by National Natural Science Foundation of China (No. 51578131), Natural Science Foundation of Jiangsu Province, China (No. BK20131287) and the Priority Academic Program Development of Jiangsu Higher Education Institutions.

#### References

- [1] Y. Sun, C. Chen, D. Shao, J. Li, X. Tan, G. Zhao, S. Yang, X. Wang, Enhanced adsorption of ionizable aromatic compounds on humic acid-coated carbonaceous adsorbents, *RSC Adv.*, 2 (2012) 10359–10364.
- [2] X. Li, J.J. Pignatello, Y. Wang, B. Xing, New insight into adsorption mechanism of ionizable compounds on carbon nanotubes, *Environ. Sci. Technol.*, 47 (2013) 8334–8341.
- [3] H Xu, Y Wan, H. Li, S. Zheng, D. Zhu, Sorption of aromatic ionizable organic compounds to montmorillonites modified by hexadecyltrimethyl ammonium and polydiallyldimethyl ammonium, *J. Environ. Qual.*, 40 (2011) 1895–1902.
- [4] E. Ayranci, O. Duman, Apparent molar volumes and isentropic compressibilities of benzene sulfonates and naphthalene sulfonates in aqueous solutions at (293.15, 303.15, 313.15, 323.15, and 333.15) K, *J. Chem. Eng. Data*, 55 (2010) 947–952.

- [5] W.C. Peng, Y. Chen, S.D. Fan, F.B. Zhang, G.L. Zhang, X.B. Fan, Use of 4,4'-dinitrostilbene-2,2'-disulfonic acid wastewater as a raw material for paramycin production, *Environ. Sci. Technol.*, 44 (2010) 9157–9162.
- [6] S. Riediker, M.J.F. Suter, W. Giger, Benzene- and naphthalene-sulfonates in leachates and plumes of landfills, *Water Res.*, 34 (2000) 2069–2079.
- [7] H.M. Gan, S. Shahir, Z. Ibrahim, A. Yahya, Biodegradation of 4-aminobenzenesulfonate by *Ralstonia* sp. PBA and *Hydrogenophaga* sp. PBC isolated from textile wastewater treatment plant, *Chemosphere*, 82 (2011) 507–513.
- [8] G. Chen, K.Y. Cheng, M. P. Ginige, A.H. Kaksonen, Aerobic degradation of sulfanilic acid using activated sludge, *Water Res.*, 46 (2012) 145–151.
- [9] V.A. Shcherbakova, K.S. Laurinavichyus, N.A. Chuvil'skaya, Y.V. Ryzhmanova, V.K. Akimenko, Anaerobic bacteria involved in the degradation of aromatic sulfonates to methane, *Appl. Biochem. Microbiol.*, 51 (2015) 209–214.
- [10] S.J. Li, L. Zhang, H.L. Chen, H. Chai, C.J. Gao, Complex extraction and stripping of H acid wastewater, *Desalination*, 206 (2007) 92–99.
- [11] M. Ravera, D. Musso, F. Gosetti, C. Cassino, E. Gamalero, D. Osella, Oxidative degradation of 1,5-naphthalenedisulfonic acid in aqueous solutions by UV-photolysis in the absence and presence of H<sub>2</sub>O<sub>2</sub>, *Chemosphere*, 79 (2010) 144–148.
- [12] A. El-Ghenemy, S. Garcia-Segura, R.M. Rodríguez, E. Brillas, M.S.E. Begrani, B.A. Abdelouahid, Optimization of the electro-Fenton and solar photoelectro-Fenton treatments of sulfanilic acid solutions using a pre-pilot flow plant by response surface methodology, *J. Hazard. Mater.*, 221–222 (2012) 288–297.
- [13] I. Arslan-Alaton, A.B. Yalabik, T. Olmez-Hanci, Development of experimental design models to predict Photo-Fenton oxidation of a commercially important naphthalene sulfonate and its organic carbon content, *Chem. Eng. J.*, 165 (2010) 597–606.
- [14] Z. Song, S.R. Edwards, R.G. Treatment of naphthalene-2-sulfonic acid from tannery wastewater by a granular activated carbon fixed bed inoculated with bacterial isolates *Arthrobacter globiformis* and *Comamonas testosteroni*, *Water Res.*, 40 (2006) 495–506.
- [15] W. Yang, A. Li, C. Fu, J. Fan, Q. Zhang, Adsorption mechanism of aromatic sulfonates onto resins with different matrices, *Ind. Eng. Chem. Res.*, 46 (2007) 6971–6977.
- [16] D. Kaušpėdienė, A. Gefenienė, E. Kazlauskienė, R. Ragauskas, A. Selskienė, Simultaneous removal of azo and phthalocyanine dyes from aqueous solutions using weak base anion exchange resin, *Water Air Soil Poll.*, 224 (2013) 1769–1780.
- [17] B.C. Pan, Q.X. Zhang, F.W. Meng, X.T. Li, X. Zhang, J.Z. Zheng, W.M. Zhang, B.J. Pan, J.L. Chen, Sorption enhancement of aromatic sulfonates onto an aminated hyper-cross-linked polymer, *Environ. Sci. Technol.*, 39 (2005) 3308–3313.
- [18] B.J. Pan, W.M. Zhang, B.C. Pan, H. Qiu, Q.R. Zhang, Q.X. Zhang, S.R. Zheng, Efficient removal of aromatic sulfonates from wastewater by a recyclable polymer: 2-naphthalene sulfonate as a representative pollutant. *Environ. Sci. Technol.*, 42 (2008) 7411–7416.
- [19] B.C. Pan, Q.X. Zhang, B.J. Pan, W.M. Zhang, W. Du, H.Q. Ren, Removal of aromatic sulfonates from aqueous media by aminated polymeric sorbents: concentration-dependent selectivity and the application. *Micropor. Mesopor. Mat.*, 116 (2008) 63–69.
- [20] H. Zhang, A. Li, J. Sun, P. Li, Adsorption of amphoteric aromatic compounds by hyper-cross-linked resins with amino groups and sulfonic groups, *Chem. Eng. J.*, 217 (2013) 354–362.
- [21] P. Ling, F. Liu, L. Li, X. Jing, B. Yin, K. Chen, A. Li, Adsorption of divalent heavy metal ions onto IDA-chelating resins: Simulation of physicochemical structures and elucidation of interaction mechanisms, *Talanta*, 81 (2010) 424–432.
- [22] X. Zhang, R. Bai, Mechanisms and kinetics of humic acid adsorption onto chitosan-coated granules, *J. Colloid Interf. Sci.*, 264 (2003) 30–38.
- [23] W. Tao, A. Li, C. Long, H. Qian, D. Xu, J. Chen, Adsorption of 5-sodiosulfisophthalic acids from aqueous solution onto poly(2-vinylpyridine) resin, *J. Hazard. Mater.*, 175 (2010) 111–116.
- [24] J. Rivera-Utrilla, M. Sánchez-Polo, The role of dispersive and electrostatic interactions in the aqueous phase adsorption of naphthalenesulphonic acids on ozone-treated activated carbons, *Carbon*, 40 (2002) 2685–2691.
- [25] P. Li, A.K. SenGupta, Sorption of hydrophobic ionizable organic compounds (HIOCs) onto polymeric ion exchangers, *React. Funct. Polym.*, 60 (2004) 27–39.
- [26] K. Nobuhiro, U. Kohei, K. Naohiro, U. Yoshikuni, Exchange characteristics of monocarboxylic acids and monosulfonic acids onto anion-exchange resins, *J. Colloid Interf. Sci.*, 271 (2004) 20–27.
- [27] Q. Xie, J. Xie, Z. Wang, D. Wu, Z. Zhang, H. Kong, Adsorption of organic pollutants by surfactant modified zeolite as controlled by surfactant chain length, *Micropor. Mesopor. Mat.*, 179 (2013) 144–150.
- [28] P.V. Bonnesen, G.M. Brown, S.D. Alexandratos, L.B. Bavoux, D.J. Presley, V. Patel, R. Ober, B.A. Moyer, Development of bifunctional anion-exchange resins with improved selectivity and sorptive kinetics for pertechnetate: batch-equilibrium experiments, *Environ. Sci. Technol.*, 34 (2000) 3761–3766.
- [29] B. Pakzadeh, J.R. Batista, Impacts of cocontaminants on the performances of perchlorate and nitrate specialty ion-exchange resins, *Ind. Eng. Chem. Res.*, 50 (2011) 7484–7493.
- [30] Y. Sun, A. Li, Z. Fei, Q. Zhang, S. Wang, Adsorption of tannin acid onto a new aminated macroporous resin from aqueous solution, *Chin. J. Polym. Sci.*, 6 (2007) 621–627.
- [31] H. Nie, G. Yang, R. Xu, F. Zhang, Z. Zhou, Z. Zhang, Thermodynamic and kinetic studies on alkoxylation of camphene over cation exchange resin catalysts, *AIChE J.*, 61 (2015) 1925–1932.
- [32] M. Lalikoğlu, A. Gök, M. K. Gök, Y.S. Aşçi, Investigation of lactic acid separation by layered double hydroxide: Equilibrium, kinetics, and thermodynamics, *J. Chem. Eng. Data*, 60 (2015) 3159–3165.
- [33] C.W. Cheung, J.F. Porter, G. McKay, Sorption kinetics for the removal of copper and zinc from effluents using bone char, *Sep. Purif. Technol.*, 19 (2000) 55–64.
- [34] Y.S. Ho, G. McKay, Pseudo-second order model for sorption processes, *Process Biochem.*, 34 (1999) 451–465.
- [35] V. Dulman, S.M. Cucu-Man, I. Bunia, M. Dumitras, Batch and fixed bed column studies on removal of Orange G acid dye by a weak base functionalized polymer, *Desalin. Water Treat.*, 57 (2016) 14708–14727.
- [36] M. Greluk, Z. Hubicki, Evaluation of polystyrene anion exchange resin for removal of reactive dyes from aqueous solutions, *Chem. Eng. Res. Des.*, 91 (2013) 1343–1351.
- [37] C. Kaya, A. Şahbaz, Ö. Arar, Ü. Yüksel, M. Yüksel, Removal of tartaric acid by gel and macroporous ion-exchange resins, *Desalin. Water Treat.*, 55 (2015) 514–521.
- [38] Z. Zhang, F. Wang, W. Yang, Z. Yang, A. Li, A comparative study on the adsorption of 8-amino-1-naphthol-3,6-disulfonic acid by a macroporous amination resin, *Chem. Eng. J.*, 283 (2016) 1522–1533.